Mission Design for a Halo Orbiter of the Earth

Robert W. Farquhar* and Daniel P. Muhonen†
NASA Goddard Space Flight Center, Greenbelt, Md.
and
David L. Richardson‡
Computer Sciences Corporation, Silver Spring, Md.

In 1978, a scientific satellite will be stationed in the vicinity of the Sun-Earth interior libration point. At this location, it will be able to continuously monitor the interplanetary medium between the Sun and the Earth. Data rates can be maintained at high levels because the libration point is only 0.01 a.u. from the Earth. However, due to the alignment of the interior libration point with the Sun as viewed from the Earth, it will be necessary to place the satellite into a "halo orbit" around the libration point. This will eliminate solar interference with downlink telemetry. It is shown that the ΔV requirement for placing a satellite into an acceptable halo orbit is quite modest. Parametric trajectory data for transfers from the Earth to the halo orbit are presented for several launch dates. Orbit selection considerations and stationkeeping requirements are also discussed.

Introduction

THE desirability of stationing a scientific satellite in the vicinity of the Sun-Earth interior libration point, L_1 (see Fig. 1), was originally discussed in 1968.[1,2] About one year later, an independent review of this concept was presented in Japan.[3,4] At the Sun-Earth L_1 point, a satellite would continously monitor the interplanetary medium upstream from the Earth. The satellite would be located far enough from the Earth (~ 0.01 a.u.) to be free from disturbances caused by the Earth's presence, but close enough to provide correlative data for measurements obtained from other spacecraft within the Earth's magnetosphere.

In 1972, it was decided to incorporate the libration point satellite concept in the International Sun-Earth Explorer (ISEE) Program.[5] The ISEE program is a joint effort of NASA and the European Space Agency (ESA) involving three spacecraft which will conduct coordinated experiments in the Earth's magnetosphere and the interplanetary medium. Two of the spacecraft, ISEE-A and B, will share a single launch vehicle that will place them into a highly eccentric Earth orbit. Once in the orbit, the separation distance between the A and B spacecraft will be controlled so they can obtain measurements of the magnetosphere's fine structure. The third spacecraft, ISEE-C, will be located in an orbit around the Sun-Earth L_1 point. A primary goal of ISEE-C is to provide continuous measurements of the interplanetary environment for the ISEE-A/B experiments. Additional ISEE-C goals include the study of cosmic rays, solar flares, and a wide variety of interplanetary phenomena. One a.u. baseline support for experiments on deep-space probes will also be provided. A complete list of ISEE-C experiments is given in Table 1. Present plans call for a launch of ISEE-C in July 1978 following the ISEE-A/B launch in October 1977.

Because ISEE-C will be the first satellite to be placed in an orbit around a libration point, the mission analyst must confront a number of new and challenging mission design problems. For instance, fuel-optimal trajectories from the Earth to the vicinity of the libration point must be specified while satisfying a variety of mission and spacecraft constraints. Orbit selection and stationkeeping operations for a libration-point mission are also quite unconventional. Details of these problems are treated in the following.

Presented as Paper 76-810 at the AIAA/AAS Astrodynamics Conference, San Diego, Calif., Aug. 18-20, 1976; submitted Aug. 21, 1976; revision received Nov. 19, 1976.
Index categories: Lunar and Interplanetary Trajectories; Spacecraft Mission Studies and Economics.

*Flight Dynamics Manager, ISEE-C. Member AIAA.
†Mission Analyst, ISEE-C.
‡Member, Technical Staff.

Spacecraft Description

The ISEE-C spacecraft is illustrated in Fig. 2. It is a spin-stabilized satellite whose basic design has evolved from the IMP series of Explorer-class spacecraft. ISEE-C is equipped with a hydrazine propulsion system for orbital and attitude control with 90 kg of fuel available for maneuvers. The S-band telemetry system will support a continuous bit rate of 2000 bps at the libration-point distance. Attitude determination will normally be accomplished with a high-resolution sun sensor (measurement accuracy $\sim 0.1°$). However, a panoramic attitude sensor will be utilized for the initial orientation of the spin axis following launch.

Orbit Selection

Before a preferred mission orbit can be identified for ISEE-C, it will be necessary to review the orbital possibilities for a satellite in the vicinity of the Sun-Earth L_1 point. In this section, the two most important families of candidate orbits around the libration point will be identified, and their applicability to the ISEE-C mission will be discussed. This discussion will be preceded by a brief summary of the principal constraints affecting the selection of the mission orbit.

Mission Constraints

An obvious problem connected with the placement of a satellite in the vicinity of the Sun-Earth L_1 point is that intense solar noise will severely limit downlink communications if the satellite is located too close to the L_1 point. Although the RF Sun at S-band subtends an angle of only 0.75° as

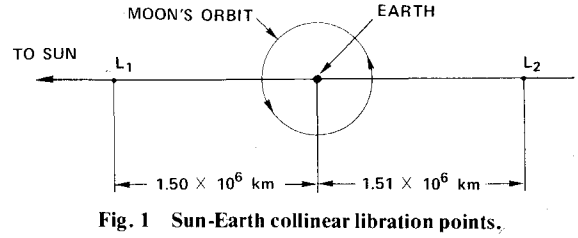

Fig. 1 Sun-Earth collinear libration points.

Table 1 ISEE-C experiments[a]

Experiment	Principal Investigator	Affiliation
Solar-Wind Plasma	S. J. Bame	Los Alamos Scientific Lab.
Magnetometer	E. J. Smith	Jet Propulsion Lab.
Low-Energy Cosmic Rays	D. Hovestadt	Max Planck Institute
Medium-Energy Cosmic Rays	T. von Rosenvinge	Goddard Space Flight Center
High-Energy Cosmic Rays	H. H. Heckman	University of California
Plasma Waves	F. L. Scarf	TRW Systems Group
Cosmic-Ray Electrons	P. Meyer	University of Chicago
Protons	R. J. Hynds	Imperial College, London
X-Rays and Electrons	K. A. Anderson	University of California
Radio Mapping	J. L. Steinberg	Meudon Observatory
Plasma Composition	K. W. Ogilvie	Goddard Space Flight Center
High-Energy Cosmic Rays	E. C. Stone	California Inst. of Technology
Ground-Based Solar Studies	J. M. Wilcox	Stanford University

[a]A gamma-ray burst experiment has also been proposed.

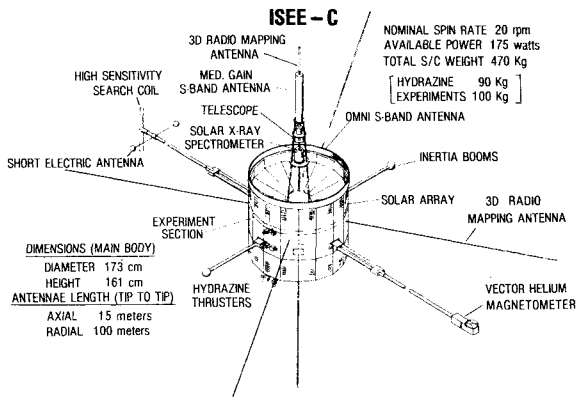

Fig. 2 ISEE-C spacecraft.

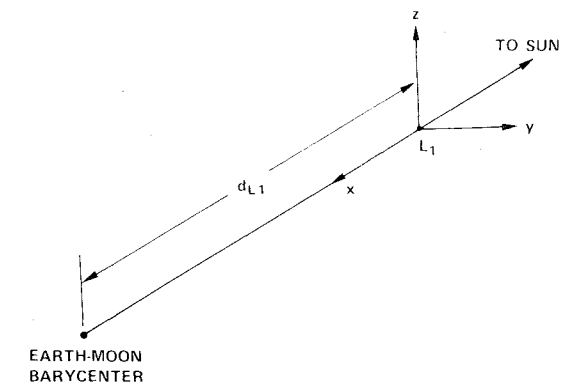

Fig. 3 Cartesian coordinate system at Sun-Earth L_1 libration point. (z-axis is perpendicular to ecliptic plane.)

viewed from the Earth, solar noise inputs to the sidelobes of ground antennas magnify the Sun's total noise contribution. Tests conducted at the Goldstone and Madrid tracking stations with 26 m antennas indicate that an offset angle of at least 3.5° will be needed to eliminate excessive solar interference with downlink communications. Therefore, the libration-point satellite must avoid an "exclusion zone" that subtends an angle of seven degrees.

When ISEE-C is stationed in its mission orbit, it has been specified that the spacecraft's spin axis will always be perpendicular ($90° \pm 1°$) to the ecliptic plane. At the same time, the Earth must lie within the beamwidth of the spacecraft's medium-gain antenna. The medium-gain antenna has a "pancake" pattern that is perpendicular to the spin axis and has a beamwidth of twelve degrees. Therefore, the angle between the Earth-spacecraft line and the ecliptic plane must always be less than six degrees.

Lissajous Orbit

If the Sun and Earth were isolated in space, the collinear libration points of this two-body system would lie on a line passing through their centers. However, prior analysis has shown that, when lunar perturbations are included, it is more accurate to locate these points on a line that passes through the Sun and the Earth-Moon barycenter.[6] A Cartesian coordinate system located on this line at the Sun-Earth L_1 point is shown in Fig. 3. Due to the Earth's orbital eccentricity, the distance, d_{L1}, between L_1 and the Earth-Moon barycenter is not constant, but the ratio of this distance to the instantaneous distance, R, between the Sun and the Earth-Moon barycenter is constant; that is, $d_{L1}/R = 0.0100109$.

Using the coordinate system of Fig. 3, it can be shown that the *linearized* equations of motion for a satellite near the Sun-Earth L_1 point are (see Ref. 1 for derivation)[§]

$$\ddot{x} - 2\dot{y} - (2B_{L1} + 1)x = 0 \tag{1a}$$

$$\ddot{y} + 2\dot{x} + (B_{L1} - 1)y = 0 \tag{1b}$$

$$\ddot{z} + B_{L1}z = 0 \tag{1c}$$

where $B_{L1} = 4.06107$. It is immediately obvious that the motion parallel to the z-axis is independent from the motion in the xy-plane and is simple harmonic. The motion in the xy-plane is coupled, and it is easily found that this motion has an oscillatory mode as well as a divergent mode. If initial conditions are chosen so that only the oscillatory mode of the xy-motion is exicted, the motion will describe a quasiperiodic orbit about the libration point. A whole family of these orbits exist, and their equations can be written in the form[¶]

$$x_n = kA_y \sin(\omega_{xy}t + \phi_{xy}) \tag{2a}$$

$$y_n = A_y \cos(\omega_{xy}t + \phi_{xy}) \tag{2b}$$

$$z_n = A_z \sin(\omega_z t + \phi_z) \tag{2c}$$

where $k = 0.309668$, $\omega_{xy} = 2.08645$, and $\omega_z = 2.01521$. In practice, the initial conditions that are required for a spacecraft to remain in a quasiperiodic orbit around the L_1 point cannot be achieved. However, the divergence from a specified quasiperiodic orbit can readily be suppressed with appropriate stationkeeping maneuvers. Details of these maneuvers are discussed later in this paper.

§The following quantites are set equal to unity: the sum of the masses of the Sun, Earth, and Moon; the mean distance between the Sun and the Earth-Moon barycenter; and the mean angular rate of the Earth-Moon barycenter around the Sun.

¶This solution has been obtained from the linearized equations of motion. Additional terms are present when nonlinearities and perturbations are taken into account.

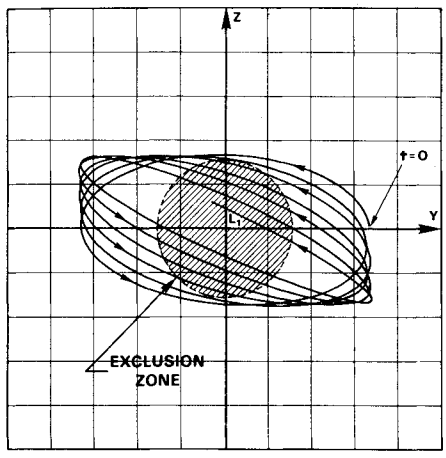

Fig. 4 Lissajous trajectory as seen from Earth, $A_y = 200{,}000$ km, $A_z = 100{,}000$ km, $\phi_{xy} = \phi_z = 0$ (grid size ~ 60,000 km).

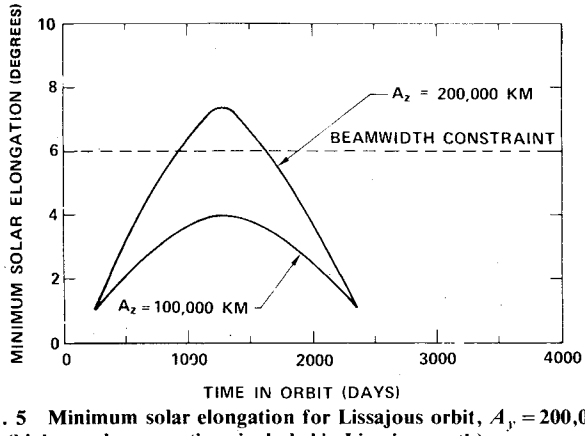

Fig. 5 Minimum solar elongation for Lissajous orbit, $A_y = 200{,}000$ km (higher-order corrections included in Lissajous path).

Because of the difference between the frequencies of the in-plane and out-of-plane oscillations, the orbits of Eqs. (2) will describe Lissajous trajectories in the yz-plane. A typical Lissajous trajectory about the Sun-Earth L_1 point is depicted in Fig. 4. Higher-order corrections (nonlinearities, perturbations) have been included in the trajectory shown in Fig. 4, but the basic character of the Lissajous path is adequately represented by Eqs. (2). The time interval for the trajectory of Fig. 4 is about three years,** which also happens to be the minimum orbital lifetime requirement for ISEE-C. Notice that this trajectory is unacceptable because it spends considerable time within the exclusion zone.

It is possible, however, to select a Lissajous orbit that will stay clear of the exclusion zone for the required three-year period. This can be accomplished with proper choices of the amplitudes, A_y and A_z, and the phase angles, ϕ_{xy} and ϕ_z. Plots of the minimum solar elongation per revolution vs time in orbit for a range of Lissajous orbits are given in Figs. 5 and 6. In Fig. 6, for example, it can be seen that with $A_y = 500{,}000$ km and $A_z = 100{,}000$ km, phase angles can be found which yield a Lissajous orbit whose minimum solar elongation will be greater than four degrees for a three-year interval. Longer periods outside the exclusion zone could be attained by selecting larger values of A_z, but A_z cannot be made too larger because of the narrow beamwidth of the spacecraft's antenna. This constraint effectively limits the maximum value of acceptable curves in Figs. 5 and 6 to six degrees.

Another way to avoid the exclusion zone while following a Lissajous path is to schedule appropriate out-of-plane

**It takes about six months to complete one revolution around the L_1 point.

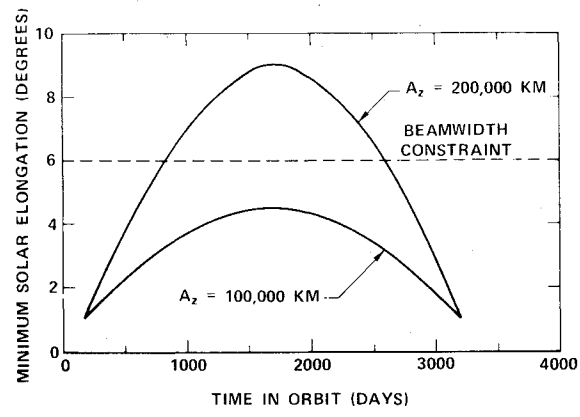

Fig. 6 Minimum solar elongation for Lissajous orbit, $A_y = 500{,}000$ km (higher-order corrections included in Lissajous path).

maneuvers to alter the period of the z-axis oscillation so that it will be synchronized with the oscillation period in the xy-plane.[1] This period control is achieved most economically by applying impulses at three-month intervals.[7] The ΔV cost for period control of a Lissajous orbit with $A_y = 200{,}000$ km and $A_z = 115{,}000$ km is approximately 20 m/sec per year.

Halo Orbit

A more appealing option for keeping ISEE-C outside of the exculsion zone while satisfying the beamwidth constraint is to employ a so-called "halo orbit." An analytical treatment of halo orbits in the restricted three-body problem was orginally presented in Ref. 8. Here it was shown that when the amplitude of the in-plane oscillation is large enough, there is a corresponding value for the amplitude of the out-of-plane oscillation that will produce a path where the fundamental frequencies are equal (i.e., $\omega_{xy} = \omega_z$). The amplitude relationship for a halo orbit around the Sun-Earth L_1 point is given by [9]

$$1.8924145 \times 10^{-13} A_z^2 - 1.6642529 \times 10^{-13} A_y^2 + 0.0712429 = 0 \tag{3}$$

where A_y and A_z are expressed in kilometers. Using Eq. (3), an easy computation reveals that halo orbits cannot exist unless $A_y > 654{,}276$ km.

Traces of a typical halo orbit are illustrated in Fig. 7. Notice that there are two families of halo orbits. The xy-projection is identical for both families, but the other projections are mirror images about the xy-plane. An isometric version of the class-2 orbit is shown in Fig. 8. The period of this orbit is about 178 days.

Parameter variations for the class-2 orbit are listed in Table 2. Due to the asymmetry of the halo orbit with respect to the xy-plane, the minimum solar-elongation angles are slightly different. A precise determination of these important angles for the orbit of Table 2 as well as some other halo orbits is given in Table 3. To satisfy mission constraints, these angles must be greater than 3.5° and less than 6.0°.

For planning purposes, the halo orbit with $A_z = 120{,}000$ km and $A_y = 666{,}672$ km has been selected as the nominal mission orbit for ISEE-C. The main reasons for choosing a halo orbit instead of a smaller-amplitude Lissajous orbit are: 1) a large-amplitude orbit minimizes the time spent in the vicinity of the exculsion zone. (It is possible that solar interference will be somewhat greater than anticipated.); 2) avoidance of the exclusion zone can be maintained indefinitely without a requirement for out-of-plane maneuvers; and 3) as will be shown in the next section, ΔV costs for orbit insertion are smaller for large-amplitude orbits.

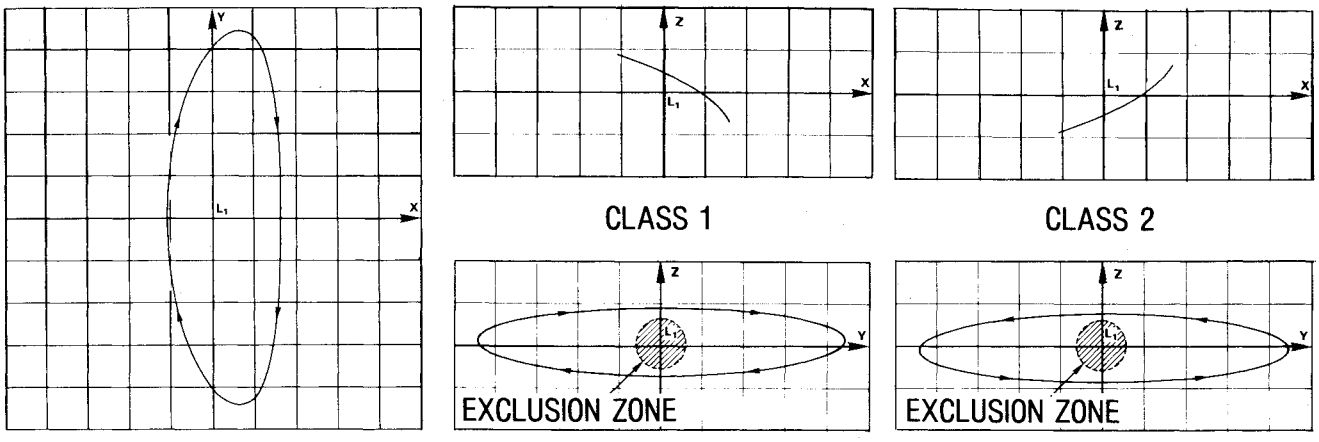

Fig. 7 Halo orbits about the Sun-Earth L_1 point, $A_z = 120{,}000$ km, $A_y = 666{,}672$ km (grid size ~ 150,000 km).

Trajectories to Halo Orbit

Spacecraft transfer trajectories from the Earth to orbits around the Sun-Earth collinear libration points are quite different from transfer trajectories utilized in Earth orbital, lunar, and interplanetary missions. This is primarily due to the fact that trajectories to the libration points will spend considerable time in a region where the gravitational effects of the Sun and the Earth are comparable. In this situation, standard analytic approximations such as the patched-conic technique break down completely, and numerical integration must be employed.

Table 2 Halo-orbit variations[a]

Time (Days)	Halo Coordinates (10^3 Km)			Earth Distance (10^6 Km)	Solar Elongation (Degrees)
	x	y	z		
0	87	663	-23	1.56	25.2
5	123	658	-2	1.52	25.6
10	155	633	19	1.48	25.3
15	181	588	40	1.44	24.1
20	202	523	59	1.40	22.1
25	218	440	76	1.36	19.2
30	229	341	91	1.32	15.6
35	236	230	101	1.29	11.3
40	240	110	108	1.27	7.0
45	241	-14	109	1.26	5.0
50	239	-138	107	1.27	7.9
55	235	-256	99	1.29	12.3
60	227	-365	88	1.33	16.5
65	215	-461	73	1.36	20.0
70	198	-540	55	1.41	22.7
75	176	-600	35	1.45	24.5
80	148	-641	14	1.49	25.4
85	115	-661	-7	1.53	25.6
90	78	-662	-28	1.57	25.0
95	38	-642	-48	1.60	23.8
100	-3	-604	-67	1.62	22.0
105	-42	-548	-84	1.64	19.8
110	-79	-476	-99	1.65	17.2
115	-111	-391	-111	1.66	14.2
120	-136	-293	-121	1.66	11.0
125	-154	-187	-128	1.67	7.8
130	-164	-75	-132	1.67	5.2
135	-166	39	-132	1.67	4.7
140	-158	152	-129	1.67	6.9
145	-143	261	-123	1.67	10.0
150	-119	361	-114	1.66	13.2
155	-89	451	-103	1.65	16.3
160	-54	527	-88	1.64	19.0
165	-15	588	-72	1.62	21.4
170	25	632	-54	1.60	23.3
175	66	658	-34	1.58	24.7
180	104	663	-13	1.54	25.5

[a] $A_z = 120{,}000$ km, $A_y = 666{,}672$ km

This section will present parametric data for transfer trajectories between an Earth parking orbit (altitude ~185 km) and an orbit around the Sun-Earth L_1 point. Two dimensional trajectories that are confined to the ecliptic plane will be examined first, and then the more realistic three-dimensional trajectories with mission constraints will be discussed.

Two-Dimensional Trajectories

Several of the most important characteristics of transfers to the vicinity of the Sun-Earth L_1 point can be observed by

Table 3 Minimum solar elongation for halo orbits

Orbit Amplitude (Km)		Minimum Solar Elongation (Degrees)	
A_z	A_y	θ_1	θ_2
80,000	659,814	3.31	3.03
100,000	662,909	4.14	3.79
120,000	666,672	4.98	4.55
140,000	671,092	5.81	5.31

Table 4 Trajectory parameters for near-optimal ecliptic-plane transfers between the Earth and planar periodic orbits around the L_1 point[a]

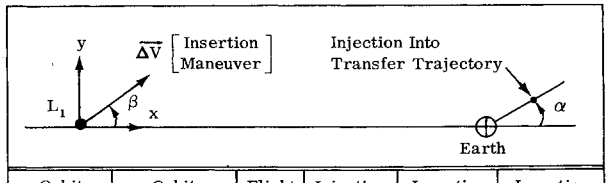

Orbit Amplitude A_y (Km)	Orbit Phase Angle ϕ_{xy} (degrees)	Flight Time ΔT (days)	Injection Angle α (degrees)	Insertion Direction β (degrees)	Insertion Magnitude ΔV (m/sec)
Fast Transfers $\Delta T < 60$ Days					
0	–	35	37	297	342
2×10^5	308	41	39	293	283
4×10^5	320	46	37	292	223
6×10^5	335	52	30	293	156
8×10^5	340	60	25	326	86
Slow Transfers 60 Days < ΔT < 120 Days					
0	–	117	13	53	279
2×10^5	108	118	14	52	209
4×10^5	110	118	14	51	137
6×10^5	110	118	13	48	62
8×10^5	127	118	2	316	13

[a] Phase angles and flight times have been varied to minimize ΔV.

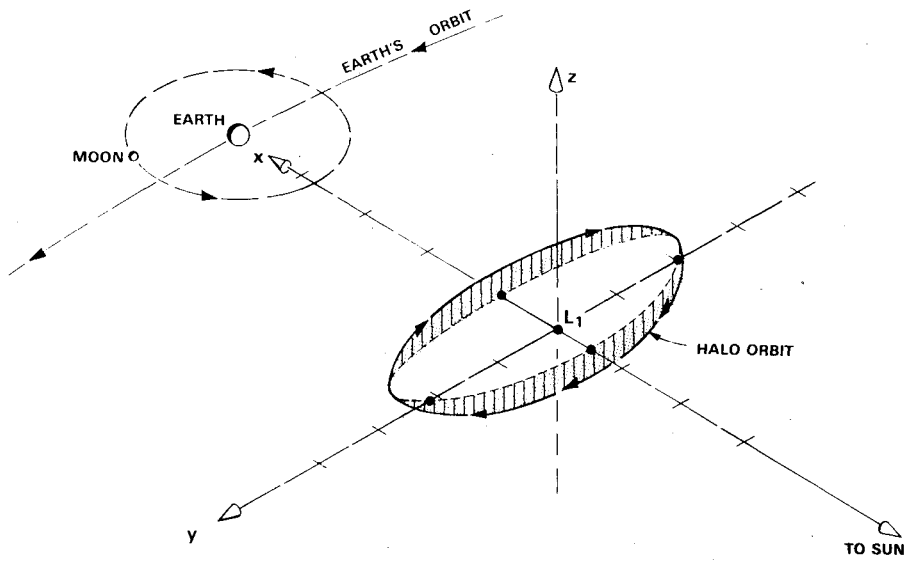

Fig. 8 Halo orbit about the Sun-Earth L_1 point, $A_z = 120{,}000$ km, $A_y = 666{,}672$ km.

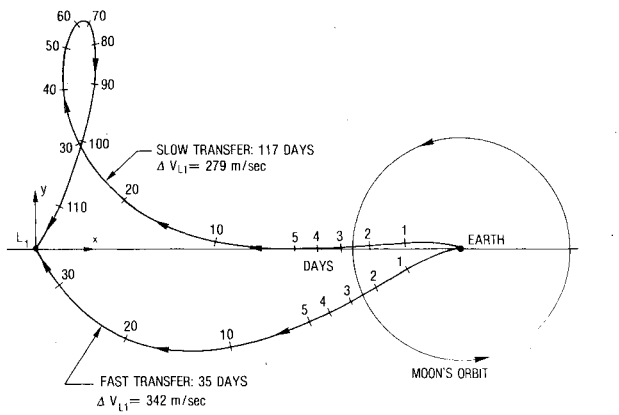

Fig. 9 Optimal ecliptic-plane transfer trajectories between the Earth and the L_1 point (flight time has been varied to minimize ΔV_{L1}).

investigating planar trajectories. Figure 9 depicts fuel-optimal examples of the two principal classes of transfers between the Earth and the Sun-Earth L_1 point.†† Optimality has been determined on the basis of the terminal maneuver at L_1 because , for the flight times considered here, the injection ΔV at the Earth parking orbit is virtually identical for every case. Although the ΔV requirement is higher for the fast transfer, the flight time is less than one-third of that required by the slow transfer. Slightly smaller ΔV costs can be achieved by using multi-impluse trajectories,[10] and greater reductions (~80 m/sec) can be gained by employing a lunar swingby.[11] However, a more effective way to reduce the ΔV cost is to simply target to an orbit around the L_1 point instead of the point itself. Near-optimal trajectories between the Earth and a planar periodic orbit around the L_1 point were found for several amplitudes of the periodic orbit. The results of this parametric investigation are given in Table 4. It is easy to see that the ΔV cost for the orbit insertion maneuver can be reduced significantly by increasing the amplitude of the periodic orbit.

Three-Dimensional Trajectories with Mission Constraints

The ISEE-C spacecraft will be launched from the Kennedy Space Center by a Delta-2914 rocket. As is the case for all real missions, a number of hardware and operational constraints must be considered when choosing a nominal transfer trajectory. The most important constraints affecting the transfer trajectory are:

1) The solar-aspect angle (spin-axis sun angle) at injection (third-stage burnout) is restricted to the range, 90° ± 15°. This is necessary for spacecraft thermal protection.

2) The Moon will be used for attitude determination immediately following injection. Due to the sensitivity limitation of the panoramic attitude sensor and attitude accuracy specifications, the Sun-Earth-Moon angle at launch should be in the range 120° ± 20° for a waning Moon (phase following full Moon). This constraint will limit the launch window to about three days per month.

3) Soon after the first midcourse correction, the spacecraft's spin axis will be oriented perpendicular (90° ± 1°) to the ecliptic. Except for certain contingency situations, this orientation will be maintained throughout the mission. At this orientation, radial thrusters will be used for maneuvers parallel to the ecliptic (all planar directions are possible because the spacecraft is spinning) and appropriate axial thrusters will be used for maneuvers perpendicular to the ecliptic. Although combinations of the radial and axial thrusters can accommodate any required thrust direction without tilting the spin axis, it is obvious that the fixed-attitude restriction will increase the ΔV requirement.

4) During the early transfer phase, the minimum solar elongation must be greater than five degrees.

As mentioned earlier, the halo orbits shown in Figs. 7 and 8 have been selected as the nominal mission orbits for ISEE-C. Three-dimensional transfer trajectories to these orbits satisfying the constraints listed previously were computed for a range of launch dates. Only slow transfers were considered because, as shown in Table 4, these transfers are more

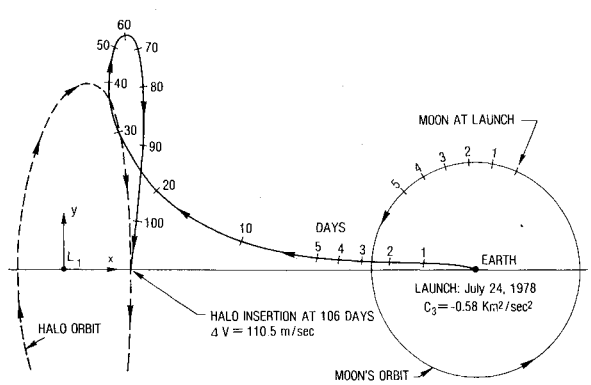

Fig. 10 Typical transfer trajectory to halo orbit (ecliptic-plane projection).

††Other classes of transfers which contain multiple loops around the Earth also exist, but multiple close Earth passages are not compatible with the objectives of the ISEE-C mission.

Table 5 Trajectory parameters for transfers to the class-1 halo orbit (A_z = 120,000 km, A_y = 666,672 km)

Launch Date	Launch Parameters			Flight Time (Days)	Minimum Solar Elongation During Early Transfer Phase (Degrees)	Halo Insertion Maneuver			
	Coast Time (minutes)	S/C Exposed to Sun[a] (minutes)	Spin-Axis Sun Angle at Injection (Degrees)			In-Plane Direction β (Degrees)	In-Plane Magnitude ΔV_{xy} (m/sec)	Out-of-Plane Magnitude ΔV_z (m/sec)	Total Magnitude ΔV (m/sec)
July 24, 1978	29.5	12.0	79.9	106	5.6	36.8	57.6	38.9	96.5
	43.8	26.0	79.0	108	6.6	34.9	44.1	-1.3	45.4
Oct. 19, 1978	11.8	0	80.5	103	5.2	38.9	72.2	61.5	133.7
	61.0	44.2	83.1	103	9.0	35.6	47.8	-6.9	54.7
Jan. 17, 1979	7.5	0	78.8	106	5.7	29.7	42.6	16.0	58.6
	65.3	49.6	88.2	104	10.9	31.6	62.4	-39.1	101.5

[a]Time from jettison of fairing to entry into earth's shadow.

Table 6 Trajectory parameters for transfers to the class-2 halo orbit (A_z = 120,000 km, A_y = 666,672 km)

Launch Date	Launch Parameters			Flight Time (Days)	Minimum Solar Elongation During Early Transfer Phase (Degrees)	Halo Insertion Maneuver			
	Coast Time (minutes)	S/C Exposed to Sun[a] (minutes)	Spin-Axis Sun Angle at Injection (Degrees)			In-Plane Direction (Degrees)	In-Plane Magnitude V_{xy} (m/sec)	Out-of-Plane Magnitude ΔV_z (m/sec)	Total Magnitude ΔV (m/sec)
July 24, 1978	20.9	5.3	88.0	106	10.5	35.5	66.9	43.6	110.5
	51.9	33.9	78.1	108	5.4	35.6	45.3	-13.0	58.3
Oct. 19, 1978	2.9	0	83.7	108	8.8	36.5	56.9	53.1	110.0
	68.7	50.4	78.1	106	6.4	36.5	41.9	1.1	43.0
Jan. 17, 1979	1.5	0	78.5	107	6.4	28.6	40.1	0.3	40.4
	73.9	56.0	79.6	105	5.3	31.9	50.5	-35.2	85.7

[a]Time from jettison of fairing to entry into earth's shadow.

economical than fast transfers and they also have smaller injection angles which makes it easier to satisfy the solar-aspect angle constraint. For planning purposes, the phase angle at halo insertion was fixed at $\phi = 90°$ (i.e., x maximum and positive, $y = 0$, z maximum), and the flight time was varied to minimize total $\Delta V (\Delta V = \Delta V_{xy} + \Delta V_z)$. Important parameters for the optimized transfer trajectories are given in Tables 5 and 6 for selected launch dates. On each launch date, optimized transfers were determined for short- and long-coast solutions,‡‡ and class-1 and class-2 halo orbits. The launch-energy requirement C_3 is not listed because, for every case, $C_3 \sim -0.6$ km^2/sec^2. A plot for a typical optimized transfer to a halo orbit is illustrated in Fig. 10.

The parameters in Tables 5 and 6 can be adjusted somewhat by varying the insertion phase angle as well as the flight time. Figure 11 shows the effect of these variations on the halo insertion maneuver and the spin-axis Sun angle for one of these cases. Notice that the ΔV cost at $\phi = 90°$ is only slightly higher than the minimum point on the curve.

Minimum ΔV for the halo-orbit insertion maneuver is not the only important factor in choosing a nominal transfer trajectory. Minimization of the time that the spacecraft is exposed to sunlight during the launch and coast phase is also highly desirable. It is even possible that a nighttime launch constraint might be necessary for adequate spacecraft thermal protection. If this constraint is imposed, all of the long-coast solutions contained in Tables 5 and 6 must be discarded. The short-coast solutions for the October and January launch dates already satisfy a nighttime launch constraint, and a satisfactory solution can be obtained for the July launch by increasing the flight time for the first case listed in Table 6 to 124 days. However, the halo-insertion ΔV cost for this case will then be increased from 111 m/sec to 175 m/sec.

On the other hand, if it is assumed that a daytime launch will be allowed, the most attractive transfer trajectory for July appears to be the second case listed in Table 5. Not only does this transfer have a very small ΔV cost, but the necessity for an out-of-plane maneuver can also be removed (i.e., $\Delta V_z = 0$) by shortening the flight time by about half a day.

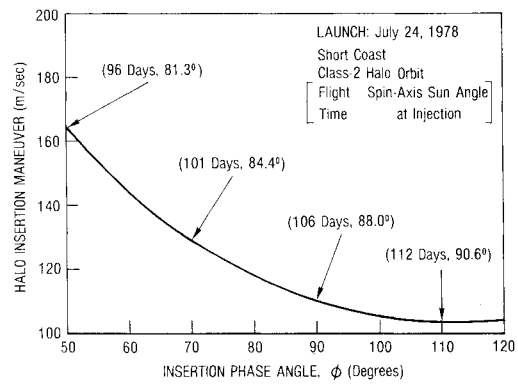

Fig. 11 Variation of optimal halo insertion maneuver (flight times have been varied to minimize ΔV at each phase angle).

Midcourse Corrections and ΔV Budget

ΔV requirements for the midcourse trajectory corrections are listed in Table 7. The first midcourse maneuver, which is scheduled for one day after launch, will remove the launch-vehicle injection dispersions. Later corrections will account for maneuver execution errors and tracking uncertainties. It

‡‡As with lunar and interplanetary transfers, there are generally two parking orbits corresponding to a fixed launch azimuth that allow injection into the transfer trajectory without a plane change. The two possibilities are termed short- and long-coast solutions depending on the time spent in the parking orbit.

Table 7 Midcourse corrections

Maneuver Execution Errors (1σ)	
Magnitude 1.5% Pointing 0.5°	
ΔV Requirement (99% Probability Level)	meters per second
MCC #1 (Launch + 1 Day)	94.7
MCC #2 (Launch + 30 Days)	9.7
MCC #3 (Launch + 70 Days)	0.7

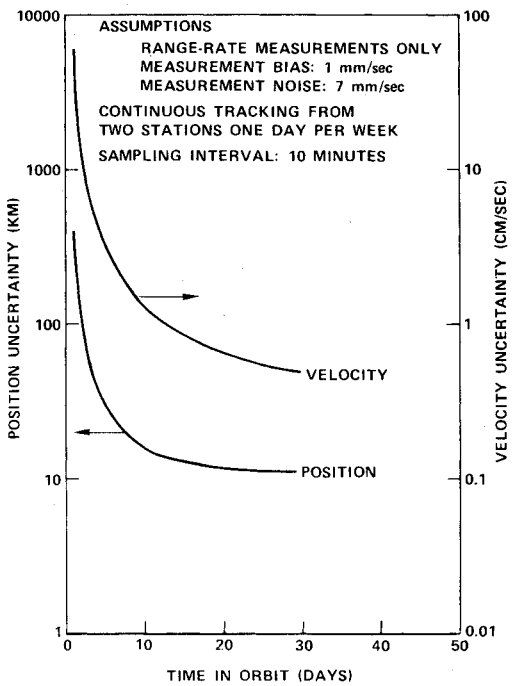

Fig. 12 Orbital accuracy (1σ) for spacecraft in halo orbit.

should be noted that the guidance strategy used to obtain the ΔV requirements given in Table 7 was not optimized.

A ΔV allocation of 300 m/sec should be sufficient for the midcourse corrections and the halo-orbit insertion maneuver. Another 100 m/sec is budgeted for attitude maneuvers, stationkeeping, and contingencies. This adds up to a total ΔV requirement of 400 m/sec, which corresponds to a hydrazine fuel loading of about 81.2 kg for ISEE-C.[§§]

Stationkeeping

As noted previously, halo orbits around the Sun-Earth L_1 point are inherently unstable, and stationkeeping maneuvers will be required for orbital maintenance. Fortunately, these maneuvers will not be needed very often, and their associated ΔV costs will be quite small (< 10 m/sec per year).[1] Intermittant maneuvers that are parallel to the xy-plane will be used to drive the ISEE-C spacecraft to a precomputed nominal halo orbit. The ΔV cost for a tight control scheme will be dependent on the accuracy of the precomputed orbit.[8] However, excessive ΔV costs can be avoided by adopting a loose control when the nominal halo orbit is not known precisely.[12]

To allow enough time for the acquisition of Sun-sensor data to satisfy the attitude-determination accuracy requirement of ± 1°, it will be necessary to separate the stationkeeping maneuvers by at least one month. This constraint is also desirable for orbit determination.[¶¶] Preliminary estimates of the position and velocity uncertainties in the halo orbit are shown in Fig. 12. These uncertainties are quite small, but they are based on a covariance analysis and may prove to be somewhat optimistic. It is suspected that it will be difficult to determine the out-of-plane components, z and $\dot{z}$, to a high degree of accuracy because of poor observability.

A rough estimate of the frequency of the stationkeeping maneuvers can be obtained from the general solution of Eq. (1). The divergent portion of this solution is given by

$$x = Ke^{\alpha t} \tag{4a}$$

$$y = -0.5345\,Ke^{\alpha t} \tag{4b}$$

where $\alpha = 2.5327$, and

$$K = 0.6257x_0 - 0.1122y_0 + 0.1737\dot{x}_0 + 0.9286\dot{y}_0 \tag{5}$$

Using Eqs. (4) and (5), and assuming that maneuver execution errors will be the dominant error source, it is easy to show that

$$\Delta V = [\dot{x}^2 + \dot{y}^2]^{1/2} \tag{6a}$$

$$\cong 2.872[0.1737\dot{x}_0 + 0.09286\dot{y}_0]e^{\alpha\Delta t} \tag{6b}$$

where Δt is the time between maneuvers. Defining $\delta V \equiv [\dot{x}_0^2 + \dot{y}_0^2]^{1/2}$, taking $\dot{x}_0 = \dot{y}_0$, and rewriting Eq. (6) in ordinary units yields

$$\Delta t = 22.95 \log (1.85\Delta V/\delta V) \text{ days} \tag{7}$$

For $\Delta V = 1.0$ m/sec and $\delta V = 0.1$ m/sec, Eq. (7) gives $\Delta t = 67$ days.

Concluding Remarks

In 1978, ISEE-C will become the first libration-point satellite. This will also be the first time that a maneuverable spacecraft will be located in an Earth orbit that is very close to escape energy ($C_3 \sim -0.6$ km^2/sec^2). With a combination of small propulsive maneuvers and lunar swingbys, it would be possible for ISEE-C to investigate any region of space within 0.01 a.u. from the Earth including the distant geomagnetic tail. This possibility could be implemented during a proposed extended mission.

References

[1] Farquhar, R.W., "The Control and Use of Libration-Point Satellites," Stanford Univ., Stanford, Calif., Report SUDAAR-350, July 1968 (reprinted as NASA TR R-346, Sept. 1970).

[2] Farquhar, R.W., "Future Missions for Libration-Point Satellites," *Astronautics & Aeronautics*, Vol. 7, May 1969, pp. 52-56.

[3] Obayashi, T., "Scientific Mission for a Helio-Stationary Spacecraft-Synchronous Planet," *Proceedings of the Eighth International Symposium on Space Technology and Science*, Tokyo, 1969, pp. 523-525.

[4] Nagatomo, M. and Matsuo, H., "Concept of a Helio-Stationary Spacecraft," *Proceedings of the Eighth International Symposium on Space Technology and Science*, Tokyo, 1969, pp. 533-538.

[5] Durney, A.C., "The International Sun-Earth Explorer (ISEE) Programme," *ESRO/ELDO Bulletin*, No. 26, Dec. 1974.

[6] Farquhar, R.W., "The Moon's Influence on the Location of the Sun-Earth Exterior Libration Point," *Celestial Mechanics*, Vol. 2, July 1970, pp. 131-133.

[§§] This calculation is based on a total spacecraft weight of 470 kg, and an average specific impulse of 215 sec for the hydrazine propulsion system.

[¶¶] Due to the sensitivity of the xy-motion to the Sun/(Earth-Moon) mass ratio, tracking data from maneuver-free arcs could lead to an improved estimate of this important constant.

[7]Farquhar, R.W., "Comments on Optimal Controls for Out-of-Plane Motion about the Translunar Libration Point," *Journal of Spacecraft and Rockets,* Vol. 8, July 1971, pp. 815-816.
[8]Farquhar, R.W. and Kamel, A.A., "Quasi-Periodic Orbits about the Translunar Libration Point," *Celestial Mechanics,* Vol. 7, June 1973, pp. 458-473.
[9]Richardson, D.L. and Cary, N.D., "Halo Orbits around the Sun-Earth Collinear Libration Points," (in preparation).
[10]D'Amario, L.D. and Edelbaum, T.N., "Minimum Impulse Three-Body Trajectories," *AIAA Journal,* Vol. 12, April 1974, pp. 455-462.
[11]Pu, C.L. and Edelbaum, T.N., "Four-Body Trajectory Optimization," *AIAA Journal,* Vol. 13, March 1975, pp. 333-336.
[12]Breakwell, J.V., Kamel, A.A. and Ratner, M.J., "Station-Keeping for a Translunar Communication Station," *Celestial Mechanics,* Vol. 10, Nov. 1974, pp. 357-373.